Energy 152 (2018) 896–905

Contents lists available at ScienceDirect

Energy

journal homepage: www.elsevier.com/locate/energy

A continuous concentration gradient flow electrical energy storage system based on reverse osmosis and pressure retarded osmosis

Rui Long*, Xiaotian Lai, Zhichun Liu, Wei Liu**

School of Energy and Power Engineering, Huazhong University of Science and Technology, 1037 Luoyu Road, Wuhan, 430074, China

ARTICLE INFO

Article history:
Received 4 December 2017
Received in revised form
2 April 2018
Accepted 5 April 2018
Available online 6 April 2018

Keywords:
Reverse osmosis (RO)
Pressure retarded osmosis (PRO)
Electrical energy storage

ABSTRACT

A continuous concentration gradient flow electrical energy storage system is presented to store the electricity generated by the renewable energy power, which consists of reverse osmosis, generating concentrated salty streams under the external power input, and pressure retarded osmosis, extracting electricity from the produced Gibbs free energy of mixing. The hybrid system is simulated on the module scale under the perfect membrane assumption. The operation parameters that impact the overall performance of the proposed system are systematically investigated. Results reveal that there exist optimal reverse osmosis and pressure retarded osmosis operation pressures leading to a maximum round-trip energy efficiency under given feed solution distribution factor. The distinct thermodynamically limiting operation regimes are identified based on analytical calculation. In the feed limited regime (FLR), a round-trip energy efficiency of 38.27% has been achieved, indicating its potential application of the proposed energy storage system.

© 2018 Elsevier Ltd. All rights reserved.

1. Introduction

Along with the fast depletion of the fossil fuels and rapid industrialization, the environment suffers much, such as global warming and the extinction of the animals due to the climate change [1]. Exploiting new and renewable energy paves a way to alleviate such issues by decreasing the consumption of traditional energy. Among them, power generated through solar and wind energy has drawn increasing attention, which offers promising candidates for electricity supply [2]. However, the intermittent nature of the renewable energy sources could not guarantee a stable output. A feasible solution is to apply electrical energy storage system (EES) in the electricity grid, thus to balance the energy output and our actual demand [3]. Up to now, 99% of the worldwide large scale electricity storage is installed in pumper hydroelectric system (PHS), which store and recover energy by pumping water into elevated reservoir and by flowing water down through a turbine [4]. The main limitation for PHS is the need for appropriate geographical conditions and it could not be installed in any place. Therefore, opportunity calls for EES is of low cost, environmentally friendly, and can also be installed without the terrain limitation.

A promising way for EES is to convert electricity into Gibbs energy of the salty solutions and then extract energy through concentration gradient technologies. As the salty solutions can be made up by dissolving NaCl in to water, which could be obtained easily, environmentally safe, and is of low cost. To produce high concentrated salty solution, distillation technologies can be applied, such as electrodialysis (ED) and reverse osmosis (RO) which are driven by external power [5–9]. To extract electricity from the produced concentrated solutions, pressure retarded osmosis (PRO) and reverse electrodialysis (RED) can be employed. In the PRO system, electricity is generated through water transfers from the diluted solution to the concentrated solution thus to drive a hydro turbine attached to a generator [10–13]. In the RED system, the ion flux transfers from the concentrated solution to the diluted one through the ion exchange membranes to produce electricity [14–18].

RO is currently the most efficient widely adopted commercial desalination technology, and as a bypass concentrated salty solutions is produced [19]. The performance of RO technology is mainly determined by the membrane properties and operating conditions. Membrane with higher salt rejection and water permeability is preferred [20]. To overcome the osmotic pressure difference, which induces water transfer from the diluted solution to the

* Corresponding author.
** Corresponding author.
E-mail addresses: r_long@hust.edu.cn (R. Long), w_liu@hust.edu.cn (W. Liu).

https://doi.org/10.1016/j.energy.2018.04.022
0360-5442/© 2018 Elsevier Ltd. All rights reserved.

concentrated one, the RO operates at higher pressure to maintain that water pierce from the high concentration solution to the lower one. To decrease the energy consumption, energy recovery device (ERD) such as pressure exchanger is employed with efficiency up to 97%, which can decrease the energy consumed as much as to 60% [21]. As one of the most promising technology to extract energy from salty solutions, the power density and energy efficiency of PRO is much higher than that of the RED [22]. Therefore, much attentions have been drawn to studying and improving the performance of the PRO systems [10]. As a membrane based technology, the membrane properties play an important role in deterring the performance. Membranes with high selectivity and large permeability is appealing. Besides, proper operation pressure can contribute to the power extracted [23].

Energy storage systems based on ED for charging and RED for discharging have been discussed preliminarily in previous literatures [24–26]. Kingsbury et al. [24] presented a rechargeable electrodialytic battery system for electricity storage based on ED and RED processes, where the cell stacks acted as an ED device and a RED device periodically, whose round-trip energy efficiency achieved 34%. Van Egmond [25] introduced a scalable energy storage system which produces concentrated and dilute solutions via an ED module and mixes these solutions to generate power through a RED module. And the internal resistance and imperfect membrane that impact the energy efficiency were researched. In their later effort [26], energy efficiency of the EES system at elevated temperatures was analyzed, and the impact of internal resistance, water transport and co-ion transport on the charging and discharging processes were systematically investigated.

In this work, we have proposed a concentration gradient flow electrical energy storage system (CGF-EES) by employing RO for "charging" process in the energy storage phase and PRO for "discharging" process in the energy extraction phase. In the energy storage phase, driven by the external power, solutions with identical concentration are changed into concentrated and diluted solutions, respectively, which means the power is stored as the Gibbs free energy of mixing, which is carried by the concentrated and diluted solutions. In the energy extraction phase, due to the osmotic pressure difference originating from different concentrations of the produced solutions, water transfers through a semipermeable membrane from the low concentration solution to the higher one, thus to generate electricity by means of a hydro-turbine. At the end of the process, the solutions out of the PRO system converges into one stream and is stored in a tank, which is subsequently used in the energy storage phase. Therefore, a closed CGF-EES is created. This paper aims at studying the energy efficiency of the proposed CGF-EES under different operational conditions. Major factors that determine the performance were researched in detail. And the optimal operation conditions have been obtained through the genetic algorithm under the maximum round-trip energy efficiency. In addition, we also investigated the working regimes of the proposed EES, thus to provide a theoretical guidance to run the CGF-EES. Finally, the practicability of the proposed electrical energy storage system was discussed and some conclusions are drawn.

2. Model development and system description

A diagrammatic sketch of the proposed RO-PRO energy storage system is depicted in Fig. 1, which includes a reverse osmosis (RO) for energy storage via converting external power into the Gibbs free energy of mixing, and pressure retarded osmosis (PRO) for electricity generation by transforming the stored energy into electricity. During the RO process where eternal power is consumed, feed solution gets concentrated and the permeate solution becomes diluted as the water transfers through the membrane. Therefore, the Gibbs free energy of mixing for the solutions increases. In the electricity generation phase, the produced solutions flow into the PRO subsystem to extract electricity. Originating from the difference of the osmotic pressure difference between different solutions and the operation pressure, transmembrane water flux gets across from the low concentration solution to the high concentration one that is then separated and drives a hydro turbine, which a generator is attached to, therefore electricity is generated.

For convenient illustration, we mark stream i as S_i with T_i, V_i, P_i, and C_i, respectively, representing its temperature, volume flow rate, pressure and salinity. Three solution tanks ($Tank_1$, $Tank_2$ and $Tank_3$) bridge the energy storage and extraction stages. Stream S_1 out of $Tank_1$ is separated into two different streams (S_2 and S_5) and then come into the RO module. Driven by the pressure pump, the pressure of Stream S_4 is increased to the operation pressure after

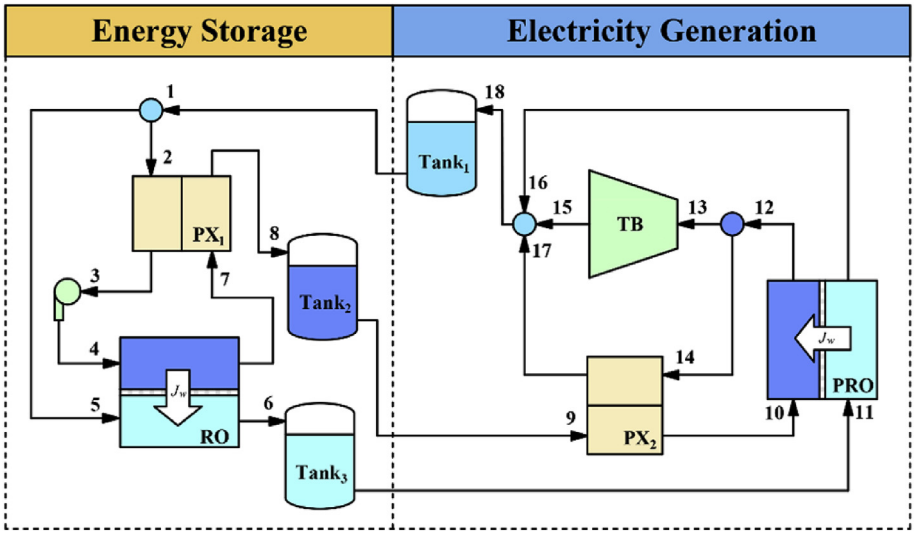

Fig. 1. Diagrammatic sketch of the proposed hybrid CGF-EES system. This system includes the energy storage section composed of a reverse osmosis system, and the energy extraction section (pressure retarded osmosis, PRO for short). In the energy storage section, driven by the external power, streams with different NaCl concentrations are produced, meanwhile, the Gibbs free energy of mixing for the solutions is augmented. In the energy extraction section, PRO module harvests the Gibbs free energy of mixing from the produced salty streams to generate electricity through a hydro turbine and the attached electricity generator. The stream i is denoted as S_i for convenience.

the pressure exchanger. The pump offers power needed for the RO process. Streams S_4 and S_5 with the same concentration but different pressure enter into the RO module. After the RO process, concentrated solution (S_7) and diluted solution (S_6) are generated, which are stored in $Tank_2$ and $Tank_3$, respectively. In order to decrease the energy needed in the energy storage procedure and augment its energy efficiency, an energy recovery device (pressure exchanger) is placed before the RO module to recover the pressure in the effluent stream of the RO system. In the electricity generation phase, Stream S_9 out of $Tank_2$ and Stream S_{11} out of $Tank_3$ run into the PRO module with pressure exchanger. After the PRO process, the effluent feed solution S_{12} separates into stream S_{13} and S_{14}, S_{14} goes into the pressure exchanger to exchange pressure with S_9. S_{13} then drives the hydro turbine and is then depressurized meanwhile electricity is generated. The solutions out of the PRO module converges into S_{18}, and then is stored in $Tank_1$ for energy storage phase. Therefore, a closed electrical energy storage system is constructed. The properties (volume flowrate, concentration, and pressure) of each stream are listed in Table 1.

2.1. Energy storage section

S_2 and S_5 enter the RO module where water transfers through the semipermeable membrane to engender concentrated and diluted solutions. The operation pressure (ΔP_{RO}) should be larger than the difference of the osmotic pressure ($\Delta\pi$) to ensure the process. The transmembrane water flux, ΔV_{RO}, equals to the decrease of volume flow rate of the feed solution. And The transmembrane water fraction, ξ_{RO}, can be defined as the percentage of the water flux across the semipermeable membrane on the inlet flow rate of the feed solution

$$\xi_{RO} = \Delta V_{RO}/V_2 \tag{1}$$

where V_2 is the inlet volume flow rate of the feed solution of the RO module with pressure exchanger. As Stream 2 is a part of stream S_1, we define a parameter α as the feed solution distribution factor. Thus we have $V_2 = \alpha V_1$. Ignoring the density changes of the salty solutions, the volume flow rate and concentration of the effluent feed solution are given by $V_7 = (1-\xi_{RO})\alpha V_1$ and $C_7 = \frac{C_1}{1-\xi_{RO}}$, respectively. The effluent volume flowrate and concentration of the permeate solution are $V_6 = (1-\alpha+\alpha\xi_{RO})V_1$ and $C_6 = \frac{1-\alpha}{1-\alpha+\alpha\xi_{RO}}C_1$, respectively.

Here we define a parameter: energy efficiency, η_{RO}, indicating the ratio between the increase of the Gibbs free energy of mixing and the external energy required, which can serve as a criterion evaluating the performance of the RO module in the energy storage phase.

$$\eta_{RO} = \frac{\Delta G_{RO}}{W_{RO}} = \frac{\Delta G_{RO,out} - \Delta G_{RO,in}}{W_{RO}} \tag{2}$$

where Gibbs free energy of mixing (ΔG) can be expressed as [27].

$$\Delta G = 2RT\left[V_H C_H \ln\frac{C_H}{C_T} + V_L C_L \ln\frac{C_L}{C_T}\right] \tag{3}$$

where C_T is the concentration of the mixed concentrated and diluted solutions. According to Eq. (3), the variation of the Gibbs free energy after the RO process is

$$\Delta G_{RO} = \nu RTV_1 C_1\left[\alpha\ln\left(\frac{1}{1-\xi_{RO}}\right) + (1-\alpha)\ln\left(\frac{1-\alpha}{1-\alpha+\alpha\xi_{RO}}\right)\right] \tag{4}$$

In order to improve the energy efficiency, a pressure exchanger with pressure recovery efficiency η_{ERD} is installed to recover the pressure of the effluent feed solution. The external energy consumed during the RO process is given by Refs. [28,29].

$$W_{RO} = \Delta P_{RO}(V_4 - \eta_{ERD}V_5) = \Delta P_{RO}\alpha V_1[1-\eta_{ERD}(1-\xi_{RO})] \tag{5}$$

Therefore, the energy efficiency in the RO process is

$$\eta_{RO} = \frac{\Delta G_{RO}}{W_{RO}} = \frac{\nu RTC_1\left[\alpha\ln\left(\frac{1}{1-\xi_{RO}}\right) + (1-\alpha)\ln\left(\frac{1-\alpha}{1-\alpha+\alpha\xi_{RO}}\right)\right]}{\Delta P_{RO}\alpha[1-\eta_{ERD}(1-\xi_{RO})]} \tag{6}$$

Table 1
Details of the flow streams in the schematic diagram of the RO-PRO hybrid system as presented in Fig. 1. Definition of the symbols can be found in the nomenclature.

Stream Number	Volume Flowrate	Concentration	Pressure
1	V_1	C_1	P_0
2	αV_1	C_1	P_0
3	αV_1	C_1	$\Delta P_{RO}+P_0$
4	αV_1	C_1	$\Delta P_{RO}+P_0$
5	$(1-\alpha)V_1$	C_1	P_0
6	$(1-\alpha+\alpha\xi_{RO})V_1$	$\frac{1-\alpha}{1-\alpha+\alpha\xi_{RO}}C_1$	P_0
7	$(1-\xi_{RO})\alpha V_1$	$\frac{C_1}{1-\xi_{RO}}$	$\Delta P_{RO}+P_0$
8	$(1-\xi_{RO})\alpha V_1$	$\frac{C_1}{1-\xi_{RO}}$	P_0
9	$(1-\xi_{RO})\alpha V_1$	$\frac{C_1}{1-\xi_{RO}}$	P_0
10	$(1-\xi_{RO})\alpha V_1$	$\frac{C_1}{1-\xi_{RO}}$	$\Delta P_{PRO}+P_0$
11	$(1-\alpha+\alpha\xi_{RO})V_1$	$\frac{1-\alpha}{1-\alpha+\alpha\xi_{RO}}C_1$	P_0
12	$(1+\xi_{PRO})(1-\xi_{RO})\alpha V_1$	$\frac{C_1}{(1-\xi_{RO})(1+\xi_{PRO})}$	$\Delta P_{PRO}+P_0$
13	$\xi_{PRO}(1-\xi_{RO})\alpha V_1$	$\frac{C_1}{(1-\xi_{RO})(1+\xi_{PRO})}$	$\Delta P_{PRO}+P_0$
14	$(1-\xi_{RO})\alpha V_1$	$\frac{C_1}{(1-\xi_{RO})(1+\xi_{PRO})}$	$\Delta P_{PRO}+P_0$
15	$\xi_{PRO}(1-\xi_{RO})\alpha V_1$	$\frac{C_1}{(1-\xi_{RO})(1+\xi_{PRO})}$	P_0
16	$V_1-(1+\xi_{PRO})(1-\xi_{RO})\alpha V_1$	$\frac{(1-\alpha)C_1}{1-(1-\xi_{RO})(1+\xi_{PRO})\alpha}$	P_0
17	$(1-\xi_{RO})\alpha V_1$	$\frac{C_1}{(1-\xi_{RO})(1+\xi_{PRO})}$	P_0
18	V_1	C_1	P_0

2.2. Energy extraction section

Streams S_9 and S_{11} with different concentrations of NaCl flow into the PRO module. A pressure exchanger is installed to exchange the low pressure of influent solution and the high pressure of the effluent solution (S_9) to produce a high pressure of S_{10}. Due to the osmotic effect, an amount of water ΔV_{PRO} transfers from the permeate solution to the feed one in the RO process. We define a transmembrane water fraction parameter $\xi_{PRO} = \Delta V_{PRO}/V_{10}$ for the PRO process. A part of the effluent of the feed solution, which equals to the transmembrane water flux, enter the hydro turbine to provide electricity

$$W_{PRO} = \Delta P_{PRO}\xi_{PRO}V_{10} = \Delta P_{PRO}\xi_{PRO}(1-\xi_{RO})\alpha V_1 \tag{7}$$

where ΔP_{PRO} is the operation pressure of the PRO module.

The energy efficiency of the PRO system can be defined by the energy output and the Gibbs free energy input [30]:

$$\eta_{PRO} = \frac{W_{PRO}}{\Delta G_{PRO}} = \frac{\Delta P_{PRO}\xi_{PRO}(1-\xi_{RO})\alpha}{\nu RTC_1\left[\alpha\ln\left(\frac{1}{1-\xi_{RO}}\right) + (1-\alpha)\ln\left(\frac{1-\alpha}{1-\alpha+\alpha\xi_{RO}}\right)\right]} \tag{8}$$

2.3. Energy efficiency of the concentration gradient energy storage system

Analysis of the aforementioned energy storage and electricity generation procedures illustrates that hybrid electrical energy storage generation system stores external power and then reclaims electricity with the round-trip energy efficiency given by:

$$\eta_{Total} = \frac{W_{PRO}}{W_{RO}} = \frac{\Delta P_{PRO}\xi_{PRO}(1-\xi_{RO})\alpha V_1}{\Delta P_{RO}\alpha V_1[1-\eta_{ERD}(1-\xi_{RO})]} = \frac{\Delta P_{PRO}\xi_{PRO}(1-\xi_{RO})}{\Delta P_{RO}[1-\eta_{ERD}(1-\xi_{RO})]} = \frac{\Delta G}{W_{RO}}\frac{W_{PRO}}{\Delta G} = \eta_{RO}\eta_{PRO} \quad (9)$$

3. Performance analysis of the concentration gradient energy storage system

3.1. Sensitivity analysis of the concentration gradient energy storage system

Based on aforementioned analysis, the parameters that affect the proposed RO-PRO system mainly consist of the RO operation pressure (ΔP_{RO}) and PRO operation pressure (ΔP_{PRO}), and the feed solution distribution factor (α). Therefore, we conduct a systematic investigation on their impacts on the performance of the RO-PRO system to give a preliminary insight into its overall performance. In the analysis, the volume flow rate, temperature, and concentration of the mainstream are fixed.

Fig. 2 shows the impacts of RO operation pressure on the performance of the proposed RO-PRO energy storage system and its subsystems. We can see that the energy efficiency of the RO, PRO and the proposed RO-PRO system all increase with increasing RO operation pressure at first, reach their maximum value, then decrease. There exist optimal RO operation pressures leading to the maximum values of the RO, PRO and round-trip energy efficiencies, respectively, as shown in Fig. 2(a). The optimal RO operation pressure leading to the maximum RO energy efficiency is less than that corresponding to the maximum value of the PRO energy efficiency. As depicted in Fig. 2(b), the work consumed by the RO system, the increase of the Gibbs free energy in the energy storage stage (RO process), and the power output in the energy extraction process increase with increasing RO operation pressure. At lower RO operation pressures, the increase of the Gibbs free energy is more obvious than that of the work consumed. Therefore, the RO energy efficiency increases. At larger RO operation pressures, the work consumed in the RO process increases much more dramatically. Whereas, the increase of the Gibbs free energy is much slow. Therefore, the RO energy efficiency decreases. The transmembrane water flux of the RO and PRO system increases nearly linearly with increases RO process, as shown in Fig. 2(c). Larger transmembrane water flux of the RO system leads to less volume flow rate of the inlet flow rate of the feed solution in PRO system. According to its definition, the transmembrane water fraction of the PRO system increases dramatically at higher RO operation pressures. The power output of the PRO system is the product of the transmembrane water flux and the PRO operation pressure, power output exhibits the same trend with the transmembrane water flux. As illustrated in Fig. 2(b), at larger RO operation pressures, the inlet Gibbs free energy of the PRO system increases much obviously, the energy efficiency of the PRO system decreases. Therefore, the PRO energy efficiency has a maximum value, and so does the round-trip energy efficiency of the hybrid RO-PRO system, as shown in Fig. 2(a).

Fig. 3 shows the impacts of PRO operation pressure on the

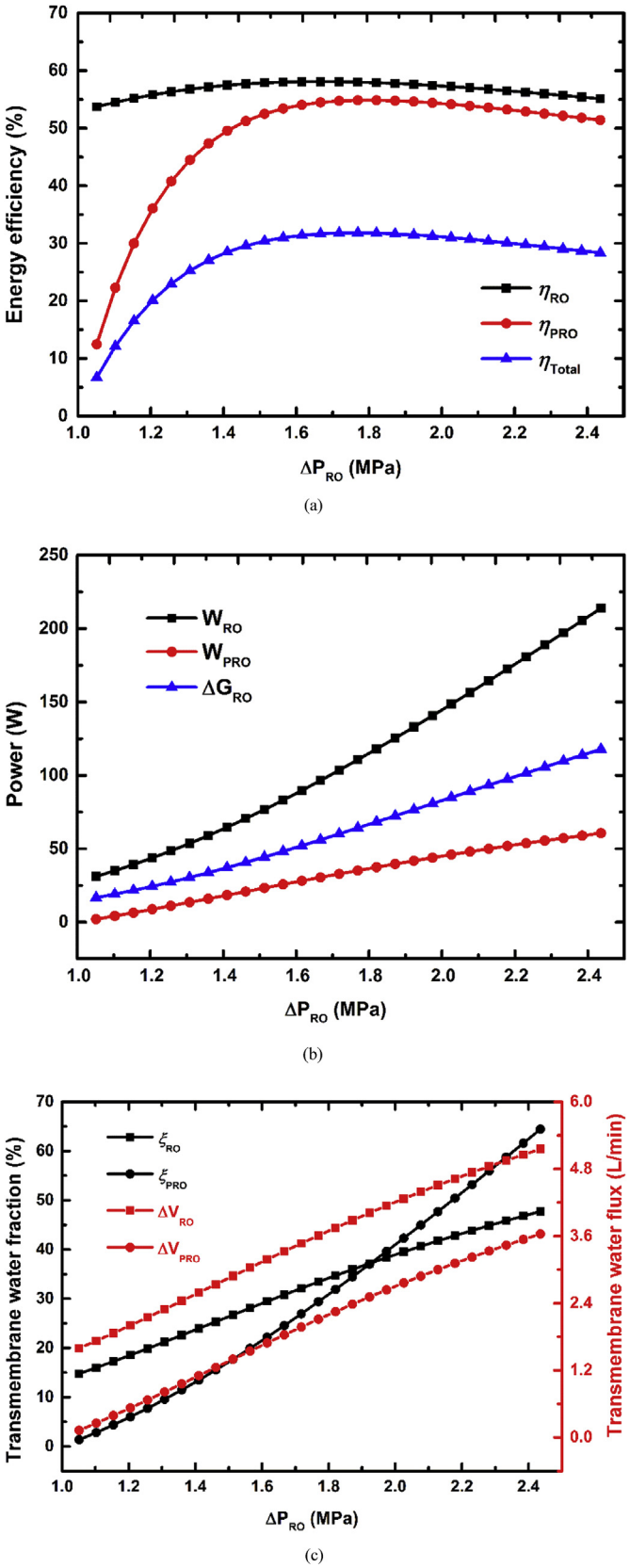

Fig. 2. Impacts of the RO operation pressure on the energy efficiency (a), power (b), and transmembrane water flux and its fraction (c) of the hybrid RO-PRO system and its subsystems, where the feed solution distribution factor in the RO system is 0.9 and the PRO operation pressure is fixed at 1 MPa.

performance of the proposed RO-PRO energy storage system and its subsystems. We can see that the performance specifications of the RO system are not impacted by the downstream PRO system as shown in the schematic diagram of the RO-PRO system. As shown in Fig. 3(a), the energy efficiency of the PRO system increases with increasing PRO operation pressure first, reaches its maximum value, then decreases. There exists an optimal PRO operation pressure leading to the maximum PRO energy efficiency. As the round-trip energy efficiency is multiplatinum of the RO and PRO energy efficiencies, it also presents a maximum value. The optimal PRO operation pressure leading to the maximum PRO energy efficiency coincides with that leading to the maximum value of the maximum round-trip energy efficiency. As depicted in Fig. 3(b), the power output in the energy extraction process first increases with increasing PRO operation pressure, reaches its maximum value, then decreases. It exhibits the same trend with the PRO energy efficiency due to the fact that the transmembrane water flux of PRO system decreases with increasing PRO operation pressure (see Fig. 3(c)). Thereby there exists an optimal PRO operation pressure leading to the maximum value of the output power based on Eq. (7).

Fig. 4 shows the impacts of the feed solution distribution factor on the performance of the proposed RO-PRO energy storage system and its subsystems. We can see that the energy efficiency of the RO, PRO and the proposed RO-PRO system all increase with increasing the feed solution distribution factor (α), and more obviously at larger values of α as shown in Fig. 4(a). As depicted in Fig. 4(c), the transmembrane water flux increases with increasing α, reaches its maximum value, then decreases. According to Eq. (6), the power consumed in the RO system presents the same trend with the transmembrane water flux, which increases with increasing α, reaches its maximum value, then decreases. There exists an optimal α leading to the maximum power consumed in the RO process as shown in Fig. 4(b). As the Gibbs free energy in the energy storage stage increase with increasing α, and decreases slightly when α near 1, the energy efficiency of the RO system increases with increasing α. Based on Eq. (8), the power output in the PRO process exhibits the same trend with transmembrane water flux, which increases with increasing α, as shown in Fig. 4(b). Therefore, a large α contributes to the system overall performance.

3.2. Optimal conditions of the concentration gradient energy storage system

Genetic algorithms (GAs) have been widely used in science and engineering as adaptive algorithms for solving non-linear optimization problems [31,32]. According to the aforementioned analysis, there exists a maximum round-trip energy efficiency, which corresponds to optimal RO and PRO operation pressures under given feed solution distribution factor. In this work, with the maximum round-trip energy efficiency as the objective function, the GA method is employed to obtain optimal parameters for the proposed RO-PRO system for different mainstream flow rates (V_1), such as for the optimization of the operation pressures of RO and PRO systems. In the optimization process, the population size is 200. Number of generations is 50. The other parameter setting uses the default values in the GA tool implemented in the MATLAB software such as that crossover ratio is 0.8 the mutation ratio is 0.2. The convergence criteria is 10^{-6}. The flowchart for the optimization process is presented in Fig. 5.

As shown in Fig. 6, the optimal RO and PRO operation pressures decrease with increasing mainstream volume flow rate. The transmembrane water flux of the RO system increases with

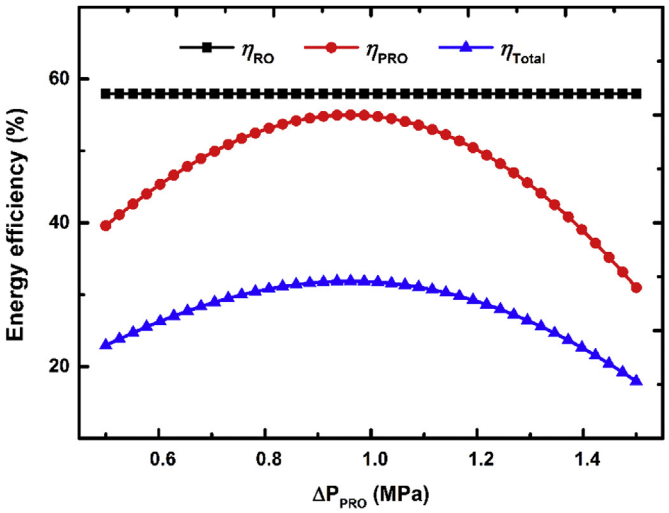

(a)

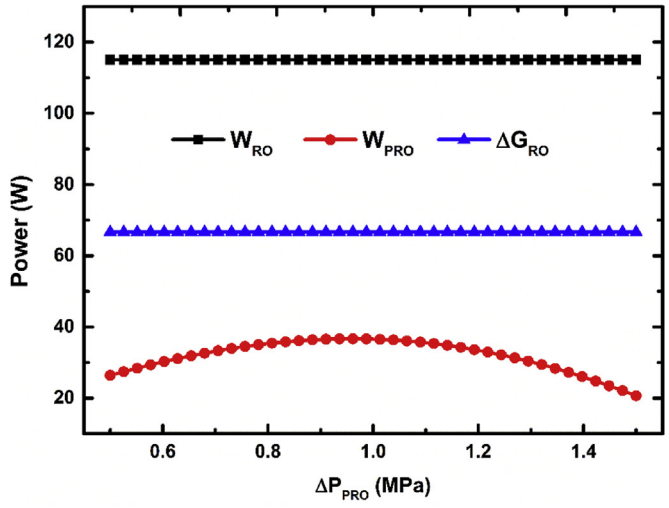

(b)

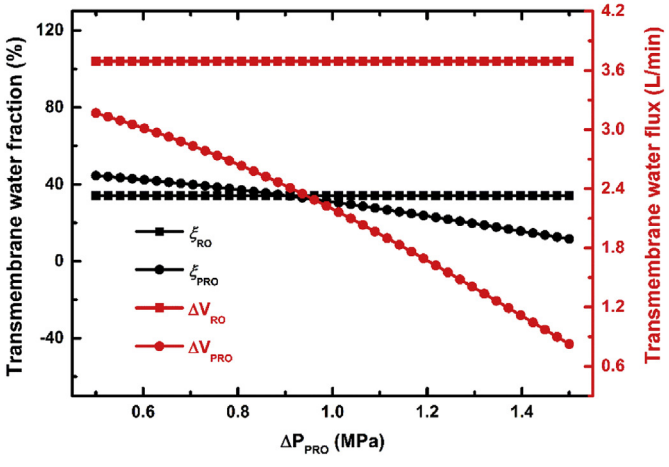

(c)

Fig. 3. Impacts of the PRO operation pressure on the energy efficiency (a), power (b), and transmembrane water flux and its fraction (c) of the hybrid RO-PRO system and its subsystems, where the feed solution distribution factor in the RO system is 0.9 and the RO operation pressure is fixed at 1.8 MPa.

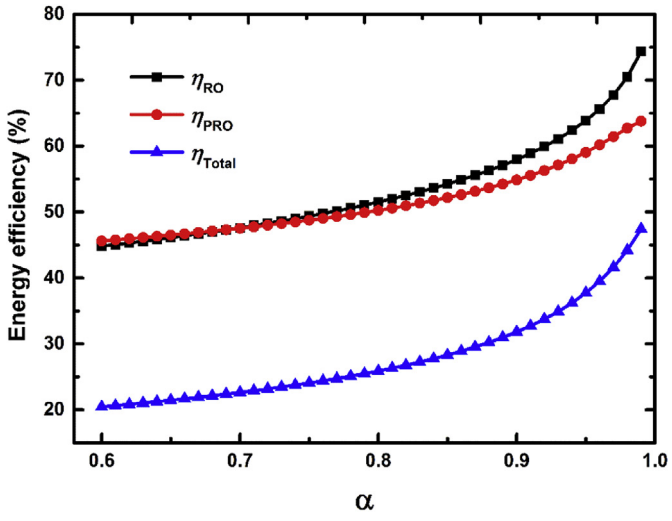

(a)

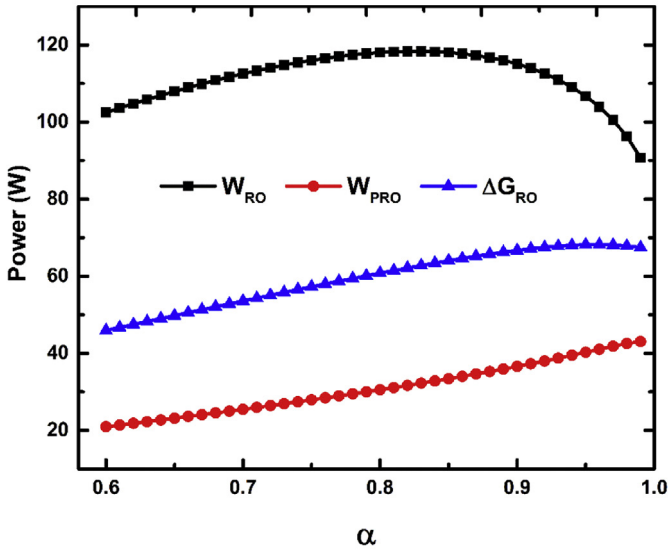

(b)

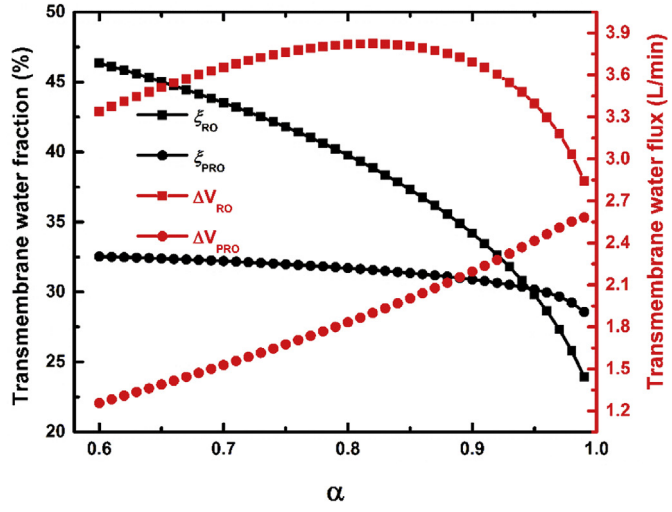

(c)

increasing mainstream volume flow rate, and that of the PRO system first increases, reaches its maximum value, then decreases. As the inlet flow rate increases more obviously than the transmembrane water flux, the transmembrane water rate decreases with increasing mainstream volume flow rate. According to Eq. (6), the power consumed in the RO process increases with increasing mainstream volume flow rate obviously at first, then much more slowly, due to the decrease of the RO operation pressure, as shown in Fig. 6(c). The power output in the PRO system presents the same trend as the transmembrane as the variation of the transmembrane water is much larger than the pressure change as depicted in Fig. 6(b). Meanwhile, the stored the Gibbs free energy of mixing first increase with increasing mainstream volume flow rate, reaches its maximum value, then decreases. Therefore, the maximum round-trip energy efficiency and its corresponding RO energy efficiency and PRO energy efficiency all decrease with increasing mainstream volume flow rate as shown in Fig. 6(d). The round-trip energy efficiency of the proposed system reaches 38.27% when the mainstream volume flow rate is 6 L/min.

4. Operation regimes of the hybrid RO-PRO system

The driving force of the RO process is the difference of the applied hydraulic pressure and the osmotic pressure difference. As the RO process precedes, the pressure difference decreases due to the increase of the osmotic pressure difference. The transmembrane water flux vanishes when $\Delta P_{RO} - \Delta\pi = 0$, indicating the maximum transmembrane water fraction is achieved under the given applied hydraulic pressure. Therefore, we have

$$\Delta P_{RO} = \Delta\pi = \nu RTC_1\left(\frac{1}{1-\xi_{RO}} - \frac{1-\alpha}{1-\alpha+\alpha\xi_{RO}}\right) \tag{10}$$

By solving Eq. (10), we have

$$\xi_{RO} = \frac{(2\alpha-1)\Delta P_{RO*} - 1 + \sqrt{(\Delta P_{RO*}+1)^2 - 4\alpha\Delta P_{RO*}}}{2\alpha\Delta P_{RO*}} \tag{11}$$

where $\Delta P_{RO*} = \frac{\Delta P_{RO}}{\nu RTC_1}$ indicates the dimensionless operation pressure of the RO device. Eq. (11) is the maximum transmembrane water fraction, which depends on the dimensionless operating pressure and the feed solution distribution factor.

Similarly, the driving force of water transfer in the PRO process is the difference of the osmotic pressure difference and the applied hydraulic pressure. As the PRO process precedes, the pressure difference decreases due to the decrease of the osmotic pressure difference. The process is terminated when $\Delta\pi - \Delta P_{PRO} = 0$ and no water flux can be transferred from the low concentration side to the high concentration side. The concentrations of the effluent solutions of the PRO system are

$$C_{10} = \frac{C_1}{(1+\xi_{PRO})(1-\xi_{RO})} \tag{12}$$

$$C_{16} = \frac{(1-\alpha)C_1}{(1-\alpha+\alpha\xi_{RO}) - \xi_{PRO}(1-\xi_{RO})\alpha} \tag{13}$$

The process stops as $\Delta P_{PRO} = \nu RT(C_{10} - C_{16})$. Therefore

Fig. 4. Impacts of the feed solution distribution factor on the energy efficiency (a), power (b), and transmembrane water flux and its fraction (c) of the hybrid RO-PRO system and its subsystems, where the RO and PRO operation pressures are fixed at 1.8 MPa and 1 MPa, respectively.

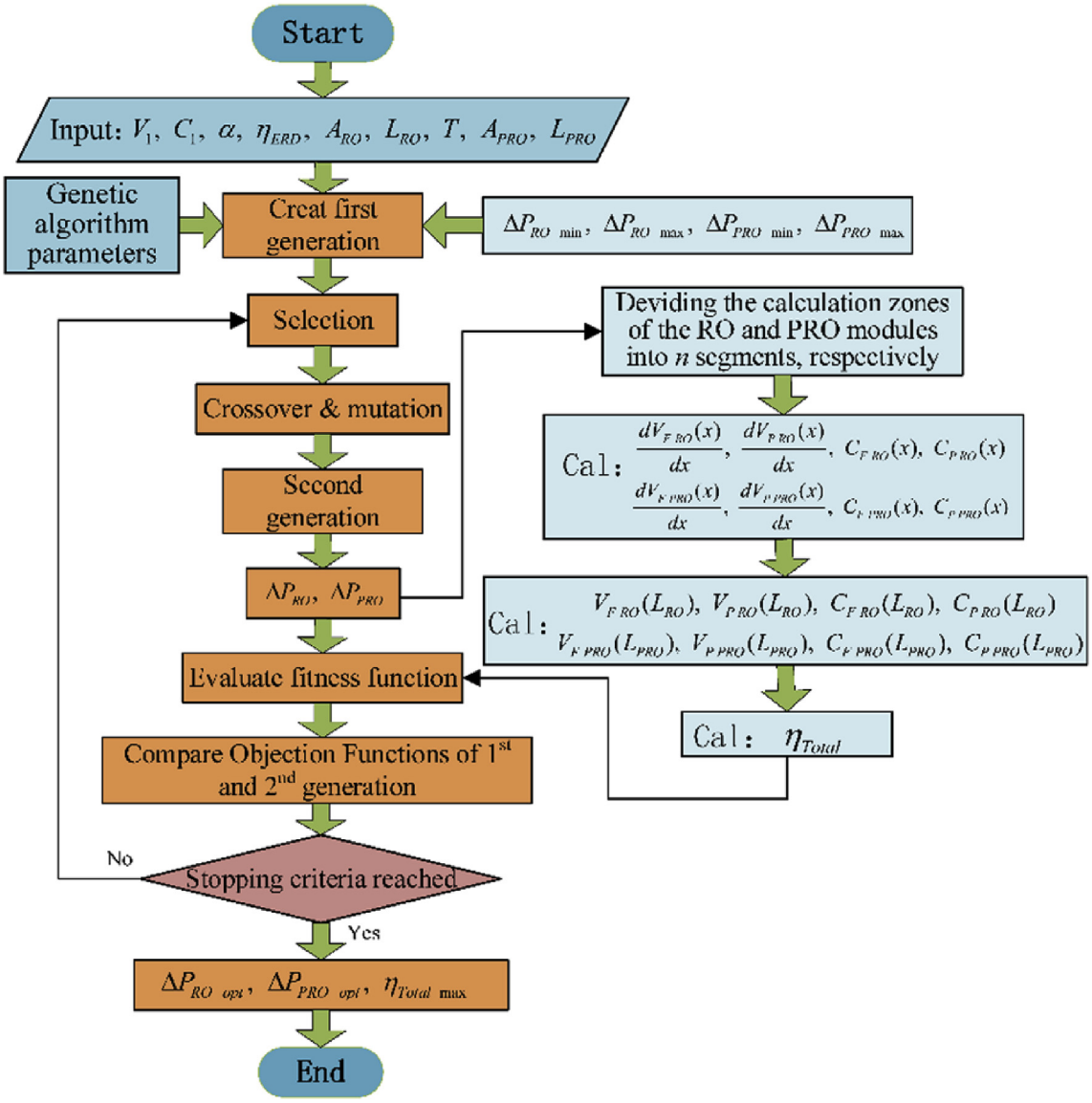

Fig. 5. Flowchart of the optimization process.

$$\Delta P_{PRO} = vRTC_1\left(\frac{1}{(1+\xi_{PRO})(1-\xi_{RO})} - \frac{(1-\alpha)}{(1-\alpha+\alpha\xi_{RO})-\xi_{PRO}(1-\xi_{RO})\alpha}\right) \tag{14}$$

By solving Eq. (14), we have the critical transmembrane water fraction of the PRO process

$$\xi_{PRO} = \frac{(1-2\alpha+2\alpha\xi_{RO})\Delta P_{PRO*}+1-\sqrt{(\Delta P_{PRO*}+1)^2-4\alpha\Delta P_{PRO*}}}{2\alpha\Delta P_{PRO}(1-\xi_{RO})} \tag{15}$$

Where $\Delta P^*_{PRO} = \frac{\Delta P_{PRO}}{vRTC_1}$ indicates the dimensionless operation pressure of the PRO device. And the maximum transmembrane water fraction of the PRO system depends on that of the RO system.

Therefore, the energy efficiencies for the RO module, PRO module, and the RO-PRO module are respectively, rewritten as

$$\eta_{RO} = \frac{\alpha\ln\left(\frac{1}{1-\xi_{RO}}\right)+(1-\alpha)\ln\left(\frac{1-\alpha}{1-\alpha+\alpha\xi_{RO}}\right)}{\Delta P^*_{RO}\alpha[1-\eta_{ERD}(1-\xi_{RO})]} \tag{16}$$

$$\eta_{PRO} = \frac{\Delta P^*_{PRO}\xi_{PRO}(1-\xi_{RO})\alpha}{\alpha\ln\left(\frac{1}{1-\xi_{RO}}\right)+(1-\alpha)\ln\left(\frac{1-\alpha}{1-\alpha+\alpha\xi_{RO}}\right)} \tag{17}$$

$$\eta_{Total} = \frac{\Delta P^*_{PRO}\xi_{PRO}(1-\xi_{RO})}{\Delta P^*_{RO}[1-\eta_{ERD}(1-\xi_{RO})]} \tag{18}$$

Fig. 7 shows the transmembrane water fraction of the RO and PRO system as a function with the mainstream volume flow rate. At lower flow rates, the membrane areas of the RO and PRO devices are sufficient for the water to pierce through. That is to say the feed solution is insufficient. The RO-PRO system operates in the FLR (feed limited regime). The transmembrane water fractions can be analytically calculated based on Eqs. (11) and (15). When the mainstream volume flow rate become larger, the RO membrane

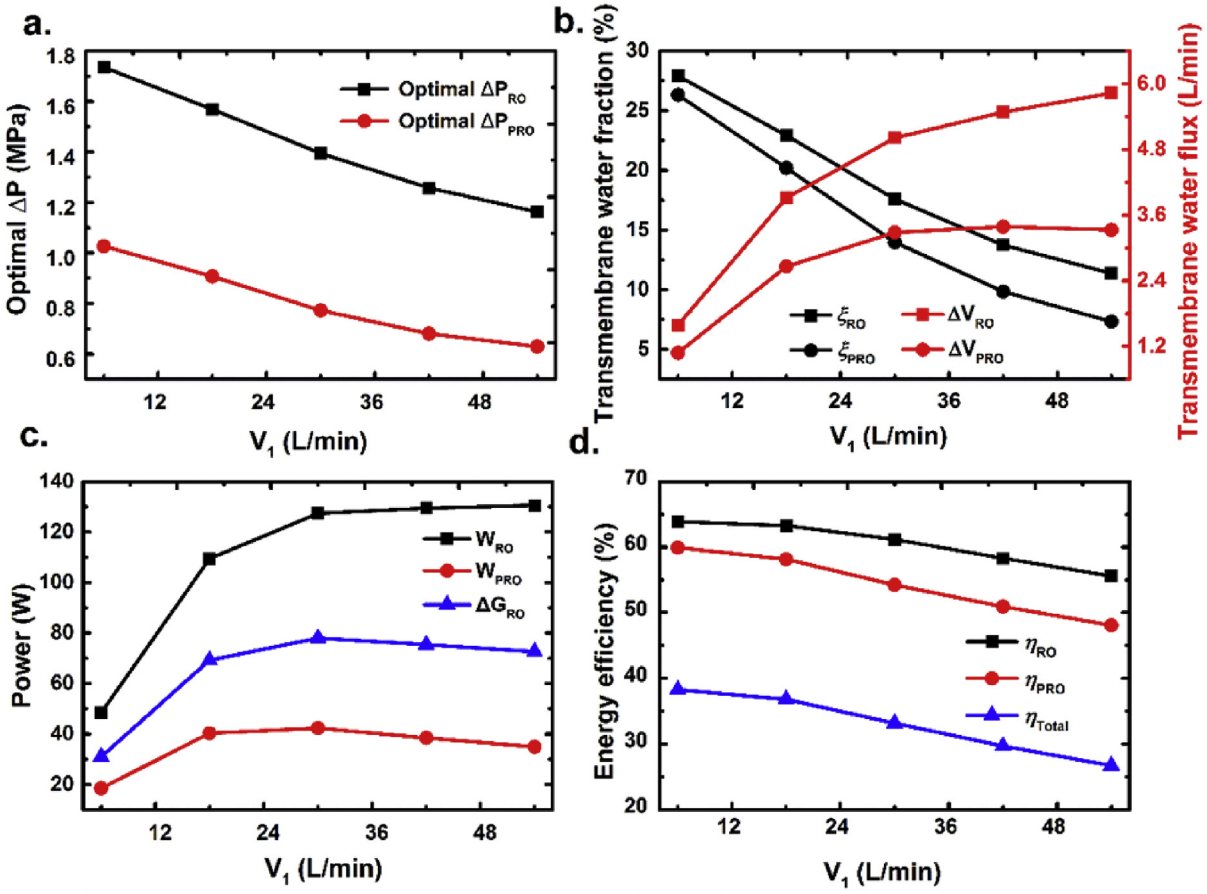

Fig. 6. Optimal RO and PRO operation pressure (a), transmembrane water flux and it fraction (b), power (c) and the system energy efficiency and its subsystem energy efficiency (d), under the optimization for the round-trip energy efficiency as a function of the mainstream volume flow rate under given feed solution distribution factor ($\alpha = 0.95$).

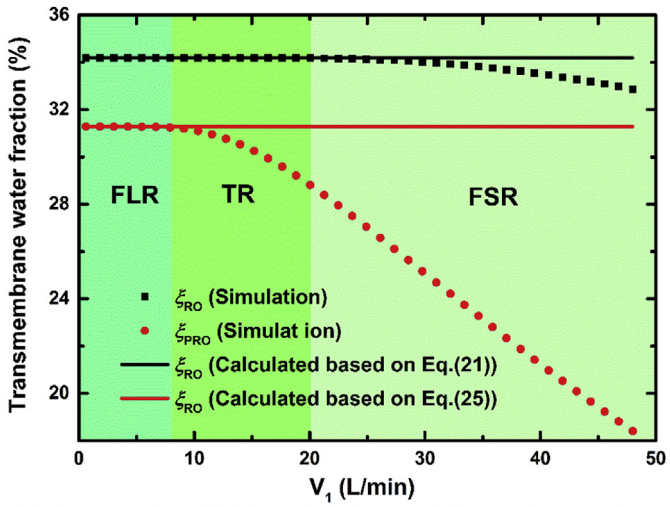

Fig. 7. Transmembrane water fraction of the RO and PRO system as a function with the mainstream volume flow rate. For comparison, those under the FLR limits are also plotted base on Eqs. (11) and (15).

area is sufficient but the PRO membrane area is insufficient. The transmembrane water fraction of the RO process can be analytically obtained whereas that of the PRO process cannot. This indicates that the RO-PRO operates in the transition regime (TR). At larger flow rates, the transmembrane water fractions both in the RO and PRO processes could not be analytically derived. It means that the RO-PRO system operates in the FSR (feed sufficient regime). In the FLR regime, the energy efficiency of the RO, PRO and RO-PRO system can be derived analytically based on Eqs. (16)–(18). The accordance of the simulation and the analytical results is depicted

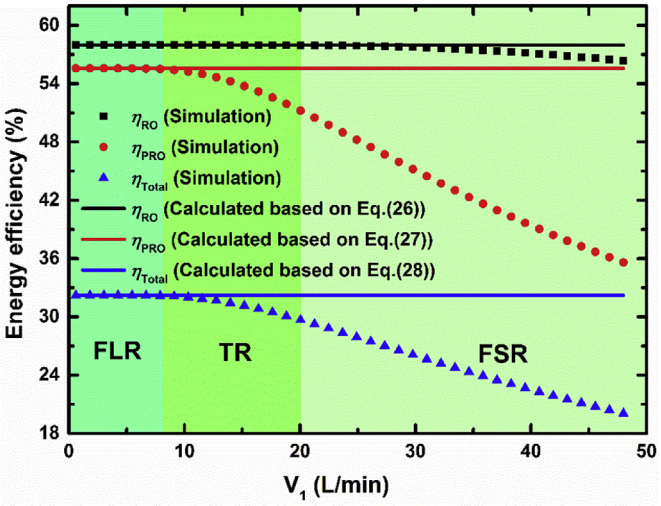

Fig. 8. Energy efficiency of the RO and PRO and the RO-PRO system as a function with the mainstream volume flow rate. For comparison, those under the FLR limits are also plotted based on Eqs. (16)–(18).

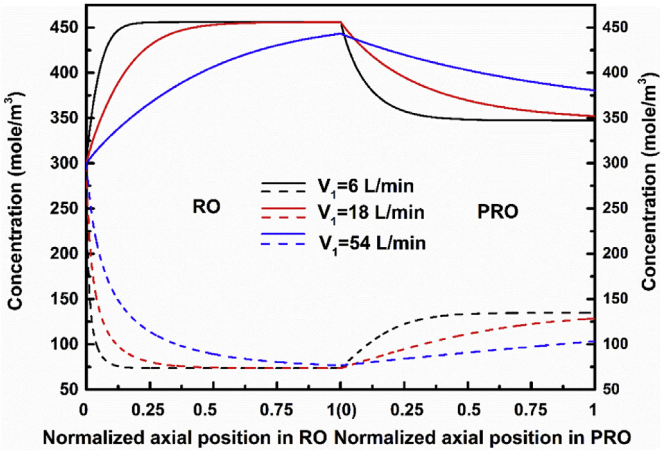

Fig. 9. Concentration profiles of the RO and PRO system under different operation regimes.

in Fig. 8.

For specific numerical cases, the concentration profiles under three different operating regimes are plotted in Fig. 9. In the FLR regime (i.e. for $V_1 = 6$ L/min), in the RO process, the concentration of the feed solution increases first, reaches its maximum value, then stays stable. The concentration of the permeant solution decreases first, reaches its minimum value, then stays stable; In the PRO process, the concentration of the feed solution decreases and that of the permeant solution increases, finally they reach their minimum or maximum value and stay unchangeable. In the transition regime (i.e. for $V_1 = 18$ L/min), in the RO process, the concentration of the feed and permeate solutions present the same trend with those in the FLR regime. In the PRO process, the concentration of the feed solution decreases while that of the permeant solution increases. In the FSR regime (i.e. for $V_1 = 54$ L/min), in the RO process, the concentration of the feed solution increases and that of the permeant solution decreases. In the PRO process, the concentration of the feed and permeate solutions present the same trend with those in the transition regime.

5. Conclusions and implications

The intrinsic low energy conversion efficiency and high energy dissipation hinder the efficient conversion of the energy storage systems. In present paper, a closed-loop hybrid electrical energy storage system consisting of a RO module and PRO module is constructed. For actual demand, the energy conversion efficiency is a critical performance objective that affects the feasibility of the energy storage system. In present study, the round-trip energy efficiency of the proposed system reaches 38.27% when working under the optimal conditions. As an efficiency of 30% could serve a criteria for possible commercial utilization [25], here the proposed energy storage system shows its advantage for potential utilization. In addition, the thermodynamic limit of the round-trip energy efficiency has also been investigated. Furthermore, for further commercial applications, a detailed cost-benefit analysis should be conducted on the system scale to inform the economic viability of the proposed hybrid electricity generation system [33].

Acknowledgements

We acknowledge the support received from the National Natural Science Foundation of China (51706076, 51736004).

Nomenclature

S_i	Stream i
T_i	Temperature of stream i (K)
V_i	Volume flow rate of stream i (L/min)
P_i	Pressure of stream i (MPa)
C_i	Concentration of stream i (mol/m^3)
ΔP	Operation pressure (MPa)
$\Delta\pi$	Osmosis pressure difference (MPa)
ΔV	Transmembrane water flux (L/min)
ΔG	Gibbs free energy of mixing (W)
W	Power (W)
R	Gas constant (8.314J·mol^{-1}·K^{-1})
A	Area m^2
L	Length m
J_w	Water flux (L/(min·m^2))

Greek Symbols

α	Feed solution distribution factor
ξ	Transmembrane water fraction
η	Energy efficiency

Subscripts

out	Outlet
in	Inlet
F	Feed flow
P	Permeate flow
Total	Hybrid system
1–18	States in the system

Superscripts

0	Initial state
*	Dimensionless

Abbreviations

RO	Reverse osmosis
PRO	Pressure retarded osmosis
EES	Electrical energy storage system
PHS	Pumper hydroelectric system
ED	Electrodialysis
RED	Reverse electrodialysis
CGF-EES	Concentration gradient flow electrical energy storage
ERD	Energy recovery device
GA	Genetic Algorithm
FLR	Feed limited regime
TR	Transition regime
FSR	Feed sufficient regime

Appendix. Modelling the Mass Transfer Characteristics in the EES System

A1. Modelling the RO process

The mass transfer characteristics in the RO process are listed as below:

$$\frac{dV_F(x)}{dx} = -\frac{A_{RO}}{L_{RO}} J_{w,RO}(C_F, C_P) \tag{A1}$$

$$\frac{dV_P(x)}{dx} = \frac{A_{RO}}{L_{RO}} J_{w,RO}(C_F, C_P) \tag{A2}$$

$$C_F(x) = C_F^0 V_F^0 \Big/ V_F(x) \tag{A3}$$

$$C_P(x) = C_P^0 V_P^0 \Big/ V_P(x) \tag{A4}$$

where $J_{w,RO} = A_{RO}(\Delta P_{RO} - \Delta\pi(x))$ and A_{RO} is the water permeability of the RO. Eqs. (A1) and (A2) are for the water transfer driven by pressure difference between the external applied pressure and the osmotic pressure difference. For simplicity, the difference of the concentrations on the membrane interface and the main solution is negligible, hence Eqs. (A3) and (A4) manifest the relation between the volume flow rate and the concentration based perfect membrane assumption that no ions pierce through the semipermeable membrane. The distributions of the volume flow rate and concentration along the flow direction can be calculated by solving the governing mass transfer Eqs. (A1) to (A4) based on four order Runge-Kutta method with the boundary conditions:

$$V_F(0) = \alpha V_1, \quad V_P(0) = (1-\alpha)V_1, \quad C_F(0) = C_P(0) = C_1 \tag{A5}$$

A2. Modelling the PRO process

According to the previous literatures, the control equations illustrating the mass transfer characteristics in the PRO process are listed as below [34]:

$$\frac{dV_F(x)}{dx} = \frac{A_{PRO}}{L_{PRO}} J_{w,PRO}(C_F, C_P) \tag{A6}$$

$$\frac{dV_P(x)}{dx} = -\frac{A_{PRO}}{L_{PRO}} J_{w,PRO}(C_F, C_P) \tag{A7}$$

$$C_F(x) = C_F^0 V_F^0 \Big/ V_F(x) \tag{A8}$$

$$C_P(x) = C_P^0 V_P^0 \Big/ V_P(x) \tag{A9}$$

where $J_{w,PRO} = A_{PRO}(\Delta\pi(x) - \Delta P_{PRO})$ and A_{PRO} is the water permeability of the PRO. Eqs. (A6) and (A7) are for the mass transfer driven by pressure difference between the osmotic pressure and the external applied pressure. Eqs. (A8) and (A9) manifest the relation between the volume flow rate and the concentration based perfect membrane assumption. The distributions of the volume flow rate and concentration along the flow direction can be calculated by solving the governing mass transfer Eqs. (A6) and (A7) based on four order Runge-Kutta method with the boundary conditions:

$$V_F(0) = V_9, \quad V_P(0) = V_{11}, \quad C_F(0) = C_9, \quad C_P(0) = C_{11} \tag{A10}$$

References

[1] Long R, Bao YJ, Huang XM, Liu W. Exergy analysis and working fluid selection of organic Rankine cycle for low grade waste heat recovery. Energy 2014;73(0):475–83.
[2] Long R, Li B, Liu Z, Liu W. Performance analysis of a solar-powered solid state heat engine for electricity generation. Energy 2015;93:165–72.
[3] Aneke M, Wang M. Energy storage technologies and real life applications – a state of the art review. Appl Energy 2016;179:350–77.
[4] Barbour E, Wilson IAG, Radcliffe J, Ding Y, Li Y. A review of pumped hydro energy storage development in significant international electricity markets. Renew Sustain Energy Rev 2016;61:421–32.
[5] Tedesco M, Hamelers HVM, Biesheuvel PM. Nernst-Planck transport theory for (reverse) electrodialysis: I. Effect of co-ion transport through the membranes. J Membr Sci 2016;510:370–81.
[6] Sarai Atab M, Smallbone AJ, Roskilly AP. An operational and economic study of a reverse osmosis desalination system for potable water and land irrigation. Desalination 2016;397:174–84.
[7] Rohlfs W, Thiel GP, Lienhard VJH. Modeling reverse osmosis element design using superposition and an analogy to convective heat transfer. J Membr Sci 2016;512:38–49.
[8] Chong TH, Loo S-L, Krantz WB. Energy-efficient reverse osmosis desalination process. J Membr Sci 2015;473:177–88.
[9] Galama AH, Saakes M, Bruning H, Rijnaarts HHM, Post JW. Seawater predesalination with electrodialysis. Desalination 2014;342:61–9.
[10] Helfer F, Lemckert C, Anissimov YG. Osmotic power with pressure retarded osmosis: theory, performance and trends – a review. J Membr Sci 2014;453:337–58.
[11] Hickenbottom KL, Vanneste J, Cath TY. Assessment of alternative draw solutions for optimized performance of a closed-loop osmotic heat engine. J Membr Sci 2016;504:162–75.
[12] Achilli A, Childress AE, Cath TY. Power generation with pressure retarded osmosis: an experimental and theoretical investigation. J Membr Sci 2009;343(1–2):42–52.
[13] Mcginnis RL, Mccutcheon JR, Elimelech M. A novel ammonia–carbon dioxide osmotic heat engine for power generation. J Membr Sci 2007;305(1–2):13–9.
[14] Vermaas DA, Saakes M, Nijmeijer K. Power generation using profiled membranes in reverse electrodialysis. Fuel Energy Abstr 2011;385–386:234–42.
[15] Güler E, Elizen R, Saakes M, Nijmeijer K. Micro-structured membranes for electricity generation by reverse electrodialysis. J Membr Sci 2014;458(6):136–48.
[16] Long R, Li B, Liu Z, Liu W. Hybrid membrane distillation-reverse electrodialysis electricity generation system to harvest low-grade thermal energy. J Membr Sci 2017;525:107–15.
[17] Long R, Li B, Liu Z, Liu W. Reverse electrodialysis: modelling and performance analysis based on multi-objective optimization. Energy 2018;151:1–10.
[18] Long R, Kuang Z, Liu Z, Liu W. Reverse electrodialysis in bilayer nanochannels: salinity gradient-driven power generation. Phys Chem Chem Phys 2018;20:7295–302.
[19] Greenlee LF, Lawler DF, Freeman BD, Marrot B, Moulin P. Reverse osmosis desalination: water sources, technology, and today's challenges. Water Res 2009;43(9):2317.
[20] Feinberg BJ, Ramon GZ, Hoek EM. Thermodynamic analysis of osmotic energy recovery at a reverse osmosis desalination plant. Environ. Sci. Technol. 2013;47(6):2982–9.
[21] Achilli A, Prante JL, Hancock NT, Maxwell EB, Childress AE. Experimental results from RO-PRO: a next generation system for low-energy desalination. Environ. Sci. Technol. 2014;48(11):6437.
[22] Yip NY, Elimelech M. Comparison of energy efficiency and power density in pressure retarded osmosis and reverse electrodialysis. Environ. Sci. Technol. 2014;48(18):11002.
[23] Amy G, Ghaffour N, Li Z, Francis L, Linares RV, Missimer T, et al. Membrane-based seawater desalination: present and future prospects. Desalination 2017;401:16–21.
[24] Kingsbury RS, Chu K, Coronell O. Energy storage by reversible electrodialysis: the concentration battery. J Membr Sci 2015;495:502–16.
[25] van Egmond WJ, Saakes M, Porada S, Meuwissen T, Buisman CJN, Hamelers HVM. The concentration gradient flow battery as electricity storage system: technology potential and energy dissipation. J Power Sources 2016;325:129–39.
[26] van Egmond WJ, Starke UK, Saakes M, Buisman CJN, Hamelers HVM. Energy efficiency of a concentration gradient flow battery at elevated temperatures. J Power Sources 2017;340:71–9.
[27] Sadeghian RB, Pantchenko O, Tate D, Shakouri A. Miniaturized concentration cells for small-scale energy harvesting based on reverse electrodialysis. Appl Phys Lett 2011;99(17):173702–3.
[28] Li M. Reducing specific energy consumption in Reverse Osmosis (RO) water desalination: an analysis from first principles. Desalination 2011;276(1):128–35.
[29] Choi J-S, Kim J-T. Modeling of full-scale reverse osmosis desalination system: influence of operational parameters. J Ind Eng Chem 2015;21:261–8.
[30] Yip NY, Elimelech M. Thermodynamic and energy efficiency analysis of power generation from natural salinity gradients by pressure retarded osmosis. Environ. Sci. Technol. 2012;46(9):5230.
[31] Long R, Li B, Liu Z, Liu W. Performance analysis of a thermally regenerative electrochemical cycle for harvesting waste heat. Energy 2015;87:463–9.
[32] Long R, Li B, Liu Z, Liu W. A hybrid system using a regenerative electrochemical cycle to harvest waste heat from the proton exchange membrane fuel cell. Energy 2015;93:2079–86.
[33] McGovern RK, Weiner AM, Sun L, Chambers CG, Zubair SM, Lienhard VJH. On the cost of electrodialysis for the desalination of high salinity feeds. Appl Energy 2014;136:649–61.
[34] Lin S, Straub AP, Elimelech M. Thermodynamic limits of extractable energy by pressure retarded osmosis. Energy Environ Sci 2014;7(8):2706–14.